# On the Linkage between Antarctic Surface Water Stratification and Global Deep-Water Temperature

RALPH F. KEELING

*Scripps Institution of Oceanography, La Jolla, California*

MARTIN VISBECK

*IFM-GEOMAR, Kiel, Germany*

(Manuscript received 29 January 2010, in final form 8 March 2011)

ABSTRACT

The suggestion is advanced that the remarkably low static stability of Antarctic surface waters may arise from a feedback loop involving global deep-water temperatures. If deep-water temperatures are too warm, this promotes Antarctic convection, thereby strengthening the inflow of Antarctic Bottom Water into the ocean interior and cooling the deep ocean. If deep waters are too cold, this promotes Antarctic stratification allowing the deep ocean to warm because of the input of North Atlantic Deep Water. A steady-state deep-water temperature is achieved such that the Antarctic surface can barely undergo convection. A two-box model is used to illustrate this feedback loop in its simplest expression and to develop basic concepts, such as the bounds on the operation of this loop. The model illustrates the possible dominating influence of Antarctic upwelling rate and Antarctic freshwater balance on global deep-water temperatures.

## 1. Introduction

A remarkable aspect of the ocean south of the Antarctic Circumpolar Current (ACC) is the low static stability of surface waters in winter (Gordon 1981). In the Weddell Sea, for example, surface waters in winter are typically fresher by 0.2 to 0.5 salinity units (g $kg^{-1}$) and colder by 2°–3°C than the deeper waters (Gordon and Huber 1990). The effects of freshening and cooling on density virtually offset one another, so that surface waters are typically only slightly less dense than the underlying waters. Salinity increases as small as 0.1 units or temperature decreases as small as 0.5° would often be sufficient to eliminate the wintertime stratification. The stratification is indeed overcome on the Antarctic continental shelf in winter, where dense waters form that feed the deep flow of Antarctic Bottom Water (AABW) into the oceans interior (Foster and Carmack 1976; Gordon et al. 1993). The occurrence of deep convection outside of the continental margins is nevertheless rare in spite of the marginal stability of the system. The large Weddell polynya of the 1970s may be one example of a breakdown in stratification induced by only modest changes in atmospheric forcing (Zwally et al. 1983; Martinson 1990; Gordon et al. 2007).

Antarctic convection plays a role in the formation of the world's deep waters, particularly the 57% of the ocean volume colder than 2°C (Gordon 1991; Orsi et al. 2001; Johnson 2008). These waters include not only AABW but also overlying waters formed from mixtures of waters of Antarctic and North Atlantic origin. By providing a pathway for exchange of heat, freshwater, and carbon dioxide between the deep ocean and the atmosphere, Antarctic convection directly impacts ocean circulation rates and the partitioning of carbon dioxide between the atmosphere and the deep sea (Gordon 1991; Sigman and Boyle 2000). The Antarctic surface layer, with its low static stability, is thus a critical feature of the global climate system (Sigman et al. 2010). A key question is whether this low static stability results from a coincidental cancelation of heat and freshwater fluxes under present climate conditions, or whether it has a more fundamental explanation.

The stratification of the Antarctic surface layer is clearly sensitive to the temperature of deep waters, which upwell

*Corresponding author address:* Ralph F. Keeling, Scripps Institution of Oceanography, UCSD, Mail Code 0244, 9500 Gilman Dr., La Jolla, CA 92093-0244.
E-mail: rkeeling@ucsd.edu

DOI: 10.1175/2011JCLI3642.1

to shallow depths south of the circumpolar current (Lumpkin and Speer 2007). Much of the surface ocean south of the ACC is cooled to the freezing point in winter, so it achieves the minimum possible temperature. This layer floats above the warmer deeper waters only because it is fresher due to precipitation and glacial ice melt. If the deep waters were sufficiently warm, this would destabilize the Antarctic water column leading to a greater tendency for deep convection. Conversely, if the deep waters were colder, this would cause the Antarctic surface layer to be more stable.

The deep-water temperature is conversely sensitive to the degree of Antarctic stratification. The global average deep-water temperature is around 1°C, notably colder than North Atlantic Deep Water (NADW), the main source of deep water outside the Antarctic (Talley et al. 2003; Johnson 2008). The difference is the result of convective cooling of deep water that is upwelled to the surface around the Antarctic, leading to the formation of AABW, which ultimately mixes into the deep ocean. In the absence of Antarctic convection, the deep oceans would presumably be warmer than present. Similarly, if convective overturning around the Antarctic were more rigorous, the deep waters would presumably be colder. The two-way influence between Antarctic stratification and deep-water temperature suggests the possibility of a feedback loop that regulates the deep-water temperature to sustain a marginally stable Antarctic surface water layer.

A similar two-way connection between Antarctic stratification and deep-water temperature has been invoked to explain the origin of slow oscillations known as "deep decoupling oscillations," which have been observed in some but not all ocean general circulation models (Winton and Sarachik 1993; Pierce et al. 1995; Haarsma et al. 2001; Meissner et al. 2008). The oscillations typically involve the cycling on a centennial-to-millennial time scale between a slow overturning mode (characterized by reduced Antarctic convection, a relatively fresh Antarctic surface, and a warming deep ocean), and a fast overturning mode (characterized by enhanced Antarctic convection, a relatively salty Antarctic surface, and a cooling deep ocean). In a time-averaged sense, these models appear to set deep-water temperature to a point yielding a partially convective Antarctic surface layer, consistent with the regulatory feedback loop described above. Prior work on this subject, however, has focused on the origin of the oscillations rather than implications of the regulatory feedback loop, which presumably could operate even if the system is not oscillatory.

As a first step in understanding the implications of this feedback loop, we develop here a simple conceptual model that allows for feedbacks between deep-water temperature, convection, and surface stratification. The model's purpose is to establish basic concepts relevant to the operation of such a feedback loop, starting with the simplest possible system that illustrates the essential behaviors. We also explore several extensions of this model to help understand how the basic concepts might need to be adapted to apply to the real ocean. We hope that concepts developed here, while derived from an idealized model, might nevertheless prove useful for understanding the behavior of more realistic systems, such as ocean–atmosphere general circulation models, which are not easily understood in terms of isolated mechanisms owing to the multitude of complex couplings that govern their behavior.

The two-way connection between surface stratification and deep-water temperature is complicated in several ways by the presence of sea ice, particularly the possibility of ice transport. To help simplify the present analysis, we assume that sea ice production and losses are locally balanced, deferring the treatment of ice transports to follow-up studies. Although models suggest that the transport of sea ice influences the thresholds for Antarctic convection and the locations and rates of AABW formation (Saenko et al. 2002; Stössel et al. 2002), the influence of Antarctic sea ice transport on deep-water salinity is nevertheless small for the modern ocean (Toggweiler and Samuels 1995b). Our model may therefore have relevance to the modern ocean despite this simplification. Sea ice transports likely had a much larger influence on deep-water salinity in the glacial ocean (Adkins et al. 2002; Keeling and Stephens 2001).

## 2. Basic model

### *a. Model description and parameters*

The basic model architecture is intended to emulate the inflow of NADW into the deep ocean and its subsequent upwelling and modification by surface process in the Antarctic. This upwelling is driven by the circumpolar westerly winds, acting on the latitude band of Drake Passage, which drives northward flow in the surface Ekman layer and raises deep waters to shallow depths south of the circumpolar current (Toggweiler and Samuels 1995a; Gnanadesikan 1999). The rate is also influenced by eddy-induced transports that partly counteract the direct wind effect, although the details of how this compensation works is a matter of ongoing research (Gnanadesikan 1999; Olbers and Visbeck 2005).

As shown in Fig. 1, the model consists of two well-mixed boxes, one representing deep water, the other surface water. Water flows into the bottom box at a specified flow rate and is extracted from the surface box at the same

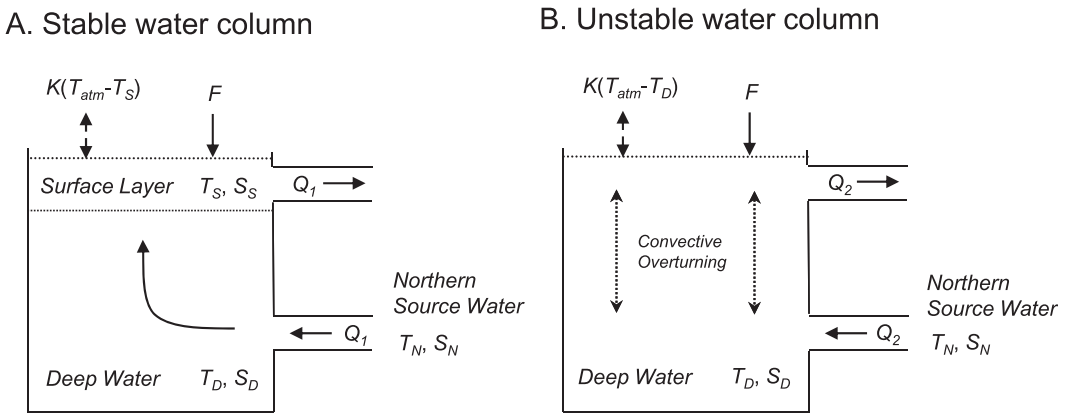


FIG. 1. Box model of upwelling system, distinguishing stratified and convective conditions.

flow. As a coarse analogy to the real ocean, the deep inflow represents the input of NADW into the deep ocean, the subsurface box represents global deep waters, and the surface box represents the ocean surface layer south of the circumpolar current.

In simple box models, the overturning circulation is typically parameterized as a function of density differences between boxes (Stommel 1961; Colin de Verdière 2007). This traditional approach is inadequate, however, for depicting mechanically driven flows, such as Antarctic upwelling. Here, following Gildor and Tziperman (2001), we prescribe the upwelling as a constant external parameter, which provides the simplest possible starting point. A first-order depiction of eddy effects, for example, would appear to require the inclusion of additional boxes (e.g., Keeling and Stephens 2001).

The surface box is modified by heat and freshwater exchanges with the atmosphere. If the net buoyancy input to the surface is positive, a stable surface layer is assumed to form. Otherwise the surface basin is assumed to be instantaneously mixed with the bottom box by convection. The representation of the surface layer is very similar to previous treatments (Welander 1982; Lenderink and Haarsma 1994), which considered the static stability of a well-mixed surface layer under freshwater and thermal forcing and water mass exchanges. Here, however, we also allow for the impact of upwelling, ice formation, and feedbacks onto deep-water properties.

The model is governed by the following external parameters:

- $T_N$, $S_N$: potential temperature and salinity of deep ''northern'' input
- $T_{\rm atm}$: effective atmospheric temperature for linear restoring
- $T_0$: potential temperature at which surface seawater freezes
- $F$: net freshwater flux from evaporation, precipitation, and glacier melt into surface layer
- $S_0$: reference salinity
- $Q_1$: upwelling flow when surface layer is present (stratified conditions)
- $Q_2$: upwelling flow when surface layer is absent (convective conditions)
- $K_0$: coupling coefficient for air–sea heat exchange under ice-free conditions and
- $\alpha, \beta$: parameters (positive definite) for linearized equation of state.

The model is ''solved'' to diagnose the following internal parameters:

- $T_D$, $S_D$: potential temperature and salinity of deep water in box and
- $T_S$, $S_S$: potential temperature and salinity of surface layer (when present).

The air–sea heat flux is parameterized according to $K(x)(T_S - T_{\rm atm})$, where $T_{\rm atm}$ is an effective atmospheric temperature (Haney 1971), and $K(x)$ is the air–sea coupling constant, assumed to depend on ice cover $x$. The air–sea heat flux is assumed to include sensible, radiative, and latent heat fluxes, including the heat required to melt precipitation. Freshwater fluxes are prescribed as equivalent salt fluxes, thus conserving water volume. We restrict our attention to cases in which $F$ is positive (precipitation plus glacier melting exceeds evaporation). A linearized equation of state is used.

The upwelling flow is assumed to be reduced ($Q_2 < Q_1$) when the water column undergoes convection. This is consistent with the notion that efficient upwelling requires the input of buoyancy at the surface to reduce the density of upwelled water (Karsten et al. 2002). The upwelling is allowed to remain finite during convective conditions, consistent with the possibility of forming

intermediate waters by the mixing of dense and less dense waters, even if buoyancy is lost from the surface.

*b. Surface water steady states*

As a first step, we evaluate the steady-state balance of the surface layer for a fixed deep-water temperature $T_D$. If a stable surface layer is present, it will be governed by the steady-state heat budget

$$Q_1(T_D - T_S) + K(x)(T_{\text{atm}} - T_S) = 0. \quad (1)$$

If $T_S$ is above the freezing point ($T_S > T_0$), then $K = K(0) = K_0$, and Eq. (1) yields the steady-state surface temperature

$$T_S = \frac{K_0 T_{\text{atm}} + Q_1 T_D}{Q_1 + K_0} \quad (T_S > T_0). \quad (2)$$

If $T_S$ is at the freezing point, then Eq. (1) effectively determines $K(x)$ or equivalently the ice coverage $x$. The surface layer will also be governed by the steady-state salinity budget:

$$-S_0 F + Q_1(S_D - S_S) = 0, \quad \text{or} \quad (3)$$

$$S_S = S_D - (F/Q_1)S_0. \quad (4)$$

The thickness of the surface layer does not enter into these steady-state relationships. We make no assumptions about the thickness of this layer, except that it is thin enough that its properties approach steady state much faster than the deep water.

A stable surface layer will exist only if the surface buoyancy forcing is positive, or equivalently that the layer is less dense than the underlying deep layer. This requires that

$$-\alpha(T_S - T_D) + \beta(S_S - S_D) < 0, \quad \text{or} \quad (5)$$

$$T_D < T_S + (\beta/\alpha)(S_D - S_S) \equiv T_{\text{neut1}}, \quad (6)$$

where $T_{\text{neut1}}$ is the deep-water temperature that yields a marginally stable surface layer. Using Eqs. (1), (3), (6), and $-\alpha(T_S - T_D) + \beta(S_S - S_D) = 0$, $T_{\text{neut1}}$ can also be written in terms of the external parameters

$$T_{\text{neut1}} = T_{\text{atm}} + (1 + g_1)\Delta T \quad (T_S > T_0), \quad \text{and} \quad (7a)$$

$$T_{\text{neut1}} = T_0 + g_1 \Delta T \equiv T_{\text{max}} \quad (T_S = T_0), \quad (7b)$$

where $\Delta T \equiv \beta S_0 F/\alpha K_0$, and $g_1 \equiv K_0/Q_1$. Here, $\Delta T$ is a temperature scale corresponding to the air–sea temperature difference that yields a buoyancy forcing equal to the freshwater input, and $T_{\text{max}}$ is the maximum deep-water temperature that permits an ice-covered surface layer; $T_{\text{max}}$ is interestingly seen to be independent of $T_{\text{atm}}$. Equations (7a) and (7b) coincide when $T_{\text{atm}} = T_0 - \Delta T$, which is the cross-over point where a marginally stable surface layer first freezes.

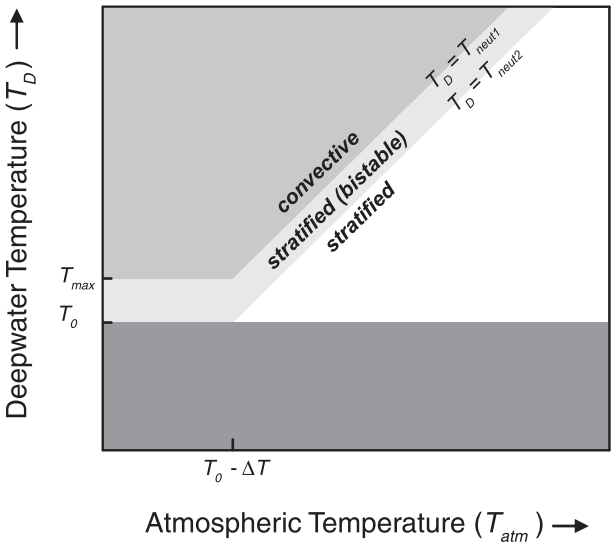


FIG. 2. Surface layer steady states of the box model, divided by shaded realms (see text). The lines bounding the realms are given by $T_D = T_{\text{neut1}}$ or $T_D = T_{\text{neut2}}$. The realm $T_D < T_0$ (darkest gray) is inaccessible because it is below the freezing point.

A convective state will exist only if the surface buoyancy forcing is negative. Assuming $T_D = T_S$ is above the freezing point $T_0$, the surface buoyancy is given by $B = g\beta S_0 F - g\alpha K_0(T_D - T_{\text{atm}})$, where $g$ is the gravitational acceleration. The requirement for convection is thus

$$\beta S_0 F - \alpha K_0(T_D - T_{\text{atm}}) < 0, \quad \text{or} \quad (8)$$

$$T_D > T_{\text{atm}} + \Delta T \equiv T_{\text{neut2}}, \quad (9)$$

where $T_{\text{neut2}}$ is the water temperature that yields zero surface buoyancy forcing.

Based on Eqs. (7) and (9), the model behavior can be divided into three realms: a convection realm ($T_D > T_{\text{neut1}}$), a stratified realm ($T_D < T_{\text{neut2}}$), and a bistable realm ($T_{\text{neut2}} < T_D < T_{\text{neut1}}$) in which convective and stratified states are both possible. These realms are shown as shaded areas on a plot of $T_D$ versus $T_{\text{atm}}$ (Fig. 2).

To this point, the analysis parallels that of Lenderink and Haarsma (1994), who considered a very similar model that neglects upwelling and freezing but includes additional parameters describing horizontal exchanges between surface boxes and prescribing a finite (rather than infinite) convective mixing rate. Allowing for these possibilities shifts the boundary between the realms slightly but not the general structure of the solution.

Lenderink and Haarsma also identified a fourth realm, previously highlighted by Welander (1982), where neither convective nor stratified steady states were achievable, a possibility that does not arise here because the freshwater flux $F$ is assumed to be positive.

In the bistable realm, the surface buoyancy forcing is positive if a surface layer is present and negative if a surface layer is absent. This mechanism of bistability is well described in the literature (Gordon and Huber 1990; Lenderink and Haarsma 1994) and will not be discussed further here. We will instead make the simplifying assumption that a stratified surface is always obtained in the bistable realm. Our purpose in making this assumption is mainly to call attention to other model behaviors that have received less attention. It is worth noting, however, that a preference for the stratified state is observed both in models (Lenderink and Haarsma 1994) and in nature (Gordon and Huber 1990), as can presumably be understood based on the greater tendency of a stratified as opposed to convective surface layer to spread horizontally.

### c. Deep-water steady states

As a second step, we consider the deep-water steady states for imposed surface water conditions. If a surface layer is present, the deep water must approach a steady state in which the temperature and salinity are equal to that of the deep input ($T_D = T_N$, $S_D = S_N$). If a surface layer is absent the deep-water temperature must approach a steady state given by

$$Q_2(T_N - T_D) + K_0(T_{\text{atm}} - T_D) = 0, \quad \text{or} \qquad (10)$$

$$T_D = \frac{g_2 T_{\text{atm}} + T_N}{g_2 + 1} \text{ (convective steady state)}, \qquad (11)$$

where $g_2 \equiv K_0/Q_2$. These two relationships describe straight lines on a plot of $T_D$ versus $T_{\text{atm}}$ as shown in Figs. 3a, 3c, and 3e.

### d. Simultaneous deep and surface steady states

The third step involves reconciling the results from the previous two sections to derive simultaneous surface and deep steady states, which are achieved only when the lines describing the deep-water steady-states lie in the appropriate realms, as shown in Figs. 3b, 3d, and 3f. A stratified state is thus achieved when the horizontal line $T_D = T_N$ lies within the stratified or bistable realms, and a convective state is achieved when the sloping line given by Eq. (10) lies within the convective realm.

As seen in Fig. 3, the structure of the steady-state solutions depends on the relative magnitude of $T_N$ versus $T_{\max}$ or equivalently on the dimensionless parameter $\chi = (T_N - T_0)/(g_1 \Delta T)$. Figures 3a and 3b show a case with $T_N < T_{\max}$ or, equivalently, $\chi < 1$. Here, the stratified steady-state line ($T_D = T_N$) and the convective steady-state line both lie entirely with the realm of stratification, as shown in Fig. 3a. So a fully stratified steady state with $T_D = T_N$ is achieved for all values of $T_{\text{atm}}$ (Fig. 3b). For this stratified steady state, the surface water temperature (Fig. 3b) is given by Eq. (2) as long as this yields a temperature above the freezing point. The transition to surface freezing occurs at $T_{\text{atm}} = T_0 - (T_N - T_0)/g_1$.

Figures 3c and 3d show a case with $T_N$ in an intermediate range $[1 < \chi < (1 + g_2 + g_1/g_2)]$. Here, the stratified steady-state line ($T_D = T_N$) crosses into the convective realm at the point $T_{\text{atm}} = T_1$, where $T_1 = T_N - (1 + g_1)\Delta T$. For $T_{\text{atm}}$ above this crossover point, the situation is the same as that considered above, and a stratified steady state is obtained. Below this point, however, a stratified steady state is not possible. A convective steady state is, however, also not possible because the convective steady-state line lies entirely within the stratified realm. To understand the behavior in this situation, suppose $T_{\text{atm}}$ is below the crossover point ($T_{\text{atm}} < T_1$) and $T_D$ is in the convective realm. Convection will then cool the deep water toward the convective steady-state line. But before $T_D$ can cool to this extent, the system will have crossed into the stratified (bistable) realm at which point the system will stratify and $T_D$ will begin to warm toward the stratified steady-state line. A small amount of warming, however, puts the system back in the convective realm where $T_D$ will again start to cool, etc. The result is that the system must oscillate between convective and stratified conditions, with $T_D$ clamped at the set point $T_{\text{neut1}}$. Depending on the atmospheric temperature, the intermittent stratified surface will either be ice covered ($T_{\text{atm}} < T_0 - \Delta T$) or ice-free ($T_{\text{atm}} > T_0 - \Delta T$).

Figures 3e and 3f show a case with $T_N$ in a high range $[\chi > (1 + g_2 + g_1/g_2)]$. Here, both the stratified and convective steady-state lines cross into the realm of convection. The situation is similar to the intermediate case, except that a fully convective (ice free) state is interposed between the frozen and unfrozen intermittent regimes.

The details of how the intermittent convection is maintained, for example, temporal and spatial characteristics, are beyond the scope of the model. What can be assessed, based on balancing the heat budget of the deep water, is the fraction of time $f$ that the system must be convective. The balance requires that the heat loss by convection $fK_0C_p(T_{\text{atm}} - T_D)$ equals the heat input from the deep inflow of "northern" water $C_p[Q_1(1 - f) + Q_2 f](T_N - T_D)$, where $C_p$ is the (volumetric) seawater

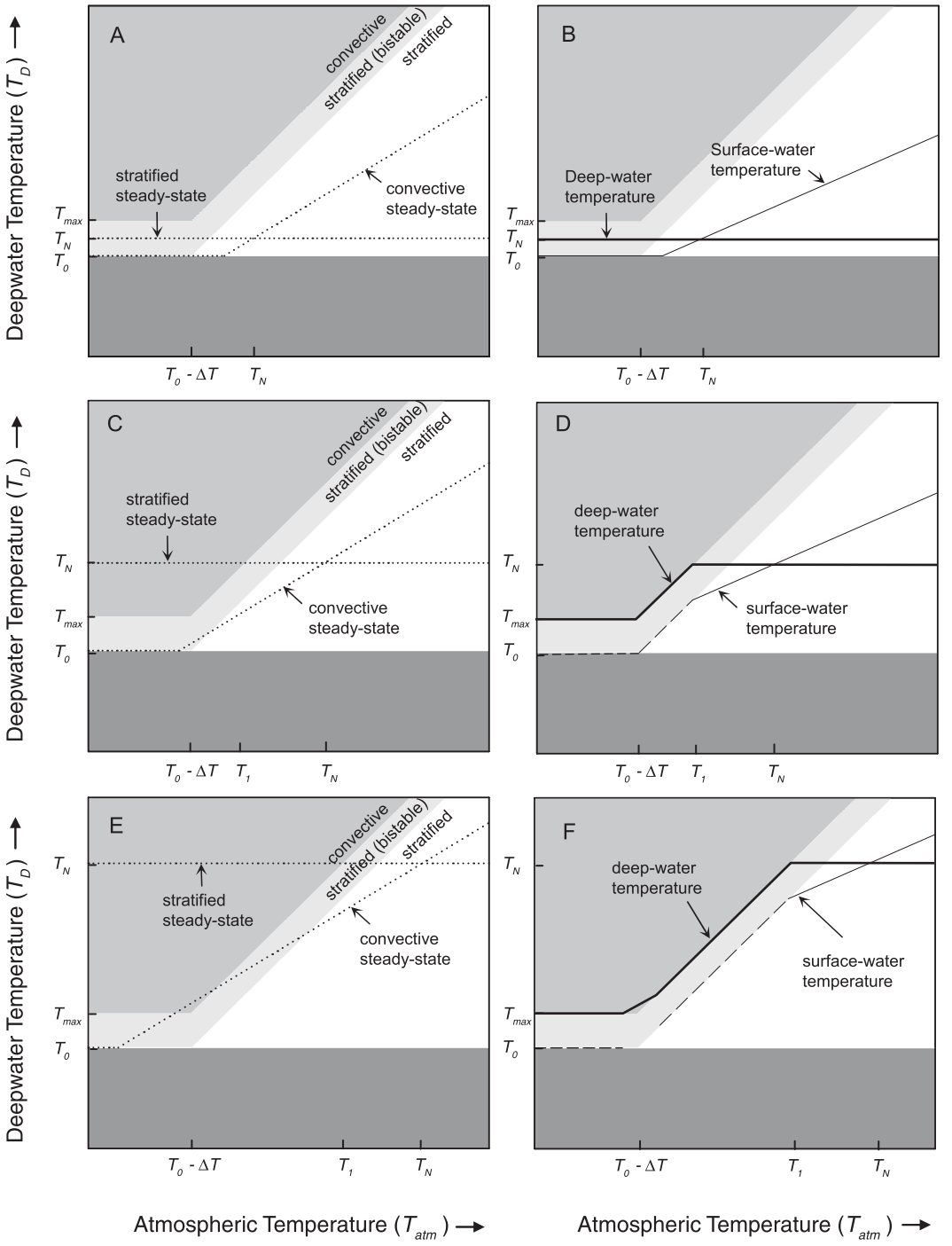


FIG. 3. Surface and deep-water steady states of the box model. (a),(c),(e) Deep-water steady-state relations (dotted lines) superimposed on surface water steady-state realms (shaded areas). Cases shown apply for different values of $T_N$. (b),(d),(f) Deep-water steady states [(a),(c),(e)] reconciled with surface water requirements and corresponding surface water steady-state temperatures. Where the surface layer is intermittent, the line is dashed.

heat capacity. Solving this balance equation for $f$ using $T_D = T_{\text{neut1}}$, $g_1 = K_0/Q_1$, and $g_2 = K_0/Q_2$ yields

$$f = \frac{T_N - T_{\text{neut1}}}{g_1(T_{\text{neut1}} - T_{\text{atm}}) + (1 - g_1/g_2)(T_N - T_{\text{neut1}})}. \quad (12)$$

The fraction $f$ depends on $T_{\text{atm}}$, both via the explicit dependence in Eq. (12) and also because $T_{\text{neut1}}$ implicitly depends on $T_{\text{atm}}$ per Eq. (7a). With an unfrozen surface, Eqs. (12) and (7a) indicate that $f$ increases as $T_{\text{atm}}$ decreases, consistent with a colder atmosphere driving more convection. With a frozen surface, Eq. (12) and (7b) indicate that $f$ decreases as $T_{\text{atm}}$ decreases. This opposite trend results because less atmospheric exposure is needed to cool the deep ocean to $T_{\max}$ as the atmosphere gets colder. In the limit $f = 1$ (all surface area undergoes convection), Eq. (12) reduces to Eq. (11), with $T_{\text{neut1}} = T_D$, as expected.

Although we have discussed the intermittent convection in temporal terms, it could also be viewed as variations in space, for example, some areas convective, some stratified. The fraction $f$ then specifies the fractional surface area undergoing convection. This spatial view forces one restriction on the interpretation of the model solution, however. Because the surface outflow will generally not be fed from the convective region, the flow $Q_2$ cannot generally be interpreted as outflow. Here, $Q_2$ could, however, be interpreted as subsurface exchange with deep water elsewhere, or it could be set to zero ($Q_2 = 0$).

A further complication applies to the fully stratified case ($\chi < 1$) considered earlier (Figs. 3a,b). This case can be divided into two subcases, depending on whether $\chi < 1/G$, where $G = \beta S_0/\alpha L$, and where $L$ is the latent heat of freezing. Here, $G$ is a dimensionless property of seawater with a nearly constant value of ~8.8 (Walin 1993). When $\chi < 1/G$ the deep-water inflow provides insufficient heat to melt the ice (e.g., snow) delivered from atmospheric precipitation, so a true steady state cannot be achieved. The precipitation must then accumulate indefinitely at the surface.

### e. Discussion of basic model

This basic model illustrates how the deep-ocean temperature in an idealized ocean can be controlled by a feedback loop that leads to a marginally stable surface layer undergoing intermittent convection in an Antarctic-like (southern) region otherwise characterized by deep upwelling. If the deep ocean is initially too warm, this triggers increased southern convection that cools the deep ocean. Conversely, if the deep ocean is initially too cold, this suppresses southern convection and allows the deep ocean to warm.

The feedback loop requires a means to warm the deep ocean in the absence of southern convection. This heat input is represented in the model as the inflow of relatively warm ''northern'' deep water. A deep-water steady state is achieved when southern convective cooling balances the heat input from northern inflow. The set point temperature ($T_{\text{neut1}}$) corresponding to this steady state is interestingly independent of the temperature of the northern inflow. In the model, the steady-state temperature of the deep water is therefore not determined by a simple blending of northern and southern end members. Instead, the set point temperature is determined by the requirement that the southern surface layer be marginally stable, that is, always on the verge of deep convection. This condition is determined [Eq. (7)] by conditions in the south, particularly the net freshwater input to the southern surface, the southern upwelling rate, and (potentially) the southern atmospheric ''temperature'' ($T_{\text{atm}}$). The bounds on this steady state can be exceeded, however, if the northern input is colder than the set point, in which case the southern surface becomes fully stratified and the deep ocean fills with pure northern water. As this bound is crossed, the control on deep-water temperature thus switches from south to north.

This basic behavior is independent of whether the southern surface is at or above the freezing point. However, if the southern surface is above the freezing point, the deep-water set point depends on the southern thermal forcing ($T_{\text{atm}}$), whereas if the southern surface is at the freezing point the set point is independent of $T_{\text{atm}}$, depending only on southern upwelling rate and freshwater forcing [Eq. (7b)]. The upwelling rate and freshwater forcing are relevant because they together determine the salinity difference between the southern surface and deep waters and thereby determine the water column static stability for a fixed deep-water temperature (given that surface temperature is clamped at the freezing point). Also, whereas the system becomes progressively more convective as the southern atmosphere gets colder under ice-free conditions, the opposite is true under freezing conditions because less convection is required to cool the deep ocean to the (fixed) set point ($T_{\text{neut1}}$) as the atmosphere gets colder.

Although our box model solutions neglect bistability of the surface layer, per Lenderink and Haarsma (1994), the model can easily be generalized to allow for such bistability. Our solutions specifically assumed that a stratified state is obtained whenever the system is in the bistable realm. If we had instead assumed that a convective state is obtained whenever the system is in the bistable realm, the

TABLE 1. Southern Ocean model parameters.

| Parameters | Symbol | Value | Reference |
|---|---|---|---|
| *T*/*S* isopycnal slope* | $\beta/\alpha$ | 16°C (g kg$^{-1}$)$^{-1}$ | |
| Reference salinity | $S_0$ | 35 g kg$^{-1}$ | |
| Precipitation rate | $F$ | 0.4 m yr$^{-1}$ | Gordon (1981) |
| Air–sea coupling | $K_0$ | 260 m yr$^{-1}$ | Haney (1971) |
| Deep-water potential temperature | $T_D$ | 1.5°C | Bolin and Stommel (1961) |
| NADW potential temperature | $T_N$ | 2.5°C | Bolin and Stommel (1961) |
| Freezing point | $T_0$ | −2°C | |
| Mean upwelling rate** | $Q_1$ | 14 m yr$^{-1}$ | |

* Based on mean slope from −2 to 2°C.
** Based on total upwelling of $15 \times 10^6$ m$^3$ s$^{-1}$ and a surface area south of the Antarctic Polar Front of $32 \times 10^{12}$ m$^2$.

same feedback loop would still have operated, with the deep-water set point simply shifting from $T_{\text{neut1}}$ to $T_{\text{neut2}}$. Alternately, if we had assumed that bistability exhibited maximum persistence, that is, the system remains stratified (or convective) until forced otherwise, the deep-water temperature would oscillate between $T_{\text{neut1}}$ and $T_{\text{neut2}}$ with a period dictated by the time to warm and cool deep ocean by convection or NADW input. In other words, the system would then exhibit a sort of deep decoupling oscillation.

## 3. Model extensions

By design, the box model depicts a very simple system that can be understood exhaustively. A key question is whether this simple system has any relevance to the real ocean. Among the potentially serious limitations of the box model is the assumption of perfect uniformity of the surface layer in space and time. To help address the question of model relevance, we now explore several extensions of the model that relax this limitation.

### *a. Variable upwelling*

We first consider an extension of the model designed to explore the impact of variable upwelling. The extension allows for explicit time dependence of the deep-water box according to

$$(V_D/A)\frac{dT_D}{dt} = Q_1(1 - f)(T_N - T_D) + fK_0(T_{\text{atm}} - T_D),$$

and (13)

$$(V_D/A)\frac{dS_D}{dt} = Q_1(1 - f)(S_N - S_D) - fFS_0, \quad (14)$$

where $V_D$ is the deep-water volume, $A$ is the Antarctic ocean surface area, $f$ is 0 or 1, depending on whether the system is stratified or convective, respectively, and we have assumed for simplicity the upwelling is zero under convective conditions ($Q_2 = 0$). Surface layer temperature and salinity are diagnosed from the steady-state relations [Eqs. (2) and (4)]. The system is solved by forward time stepping with a 0.1-yr time step, using $V_D/(A\overline{Q}_1) = 200$ yr and values of $\beta/\alpha$, $F$, $K_0$, $T_N$, and $T_0$ as given in Table 1. A new value of $f$ is diagnosed each time step based on the static stability of the surface layer in that step. To explore model behavior over a range of parameter space, $T_{\text{atm}}$ is ramped upward from an initial low value, with the ramp being sufficiently slow to ensure that the deep-water temperature maintains a quasi-steady state. In addition to carrying out runs with various constant values of $Q_1$, we also carry out runs with $Q_1$ varying randomly from year to year about the mean $\overline{Q}_1$ according to a Rayleigh probability distribution, chosen as the simplest distribution that ensures positive definite upwelling.

As shown in Fig. 4, the runs with constant upwelling conform to the steady-state solutions from the analytical model derived above. The runs with variable upwelling differ in requiring lower mean upwelling rates to achieve the same deep-water temperatures. This behavior results because the system is more prone to convection at high upwelling rates and because the steady-state involves, in all cases, relatively infrequent convection owing to the high magnitude of the air–sea coupling constant ($K_0$). The system therefore undergoes convection only for rather extreme values of the upwelling rate.

For example, let us compare the steady state with a constant upwelling rate ($Q_1$ = 60 m yr$^{-1}$) with the case with variable upwelling ($\overline{Q}_1$ = 30 m yr$^{-1}$). As seen in Fig. 4, these cases achieve similar deep-water temperatures ($T_D$ = ~1.7°C) for $T_{\text{atm}}$ = −3°C. For both cases, the time-averaged convection fraction $f$ (not shown) is ~4%. For the variable case, this requires that convection occurs only when the upwelling rate falls within the top 4% of the upwelling distribution. For a Rayleigh distribution with a mean of 30 m yr$^{-1}$, the upwelling rate defining the 4% threshold is ~60 m yr$^{-1}$. The cases therefore achieve similar deep-water temperatures because the upwelling rate marking the 4% tail of the distribution in the variable case equals the specified (constant) upwelling in the constant case. For the variable case,

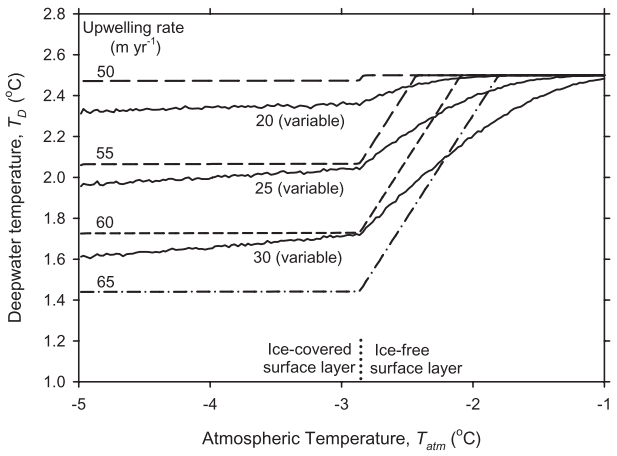


FIG. 4. Solutions to the model that include tendency terms for the deep box showing the average deep-water temperature vs effective atmospheric temperature. The three solid curves show results for variable upwelling, where the upwelling rate is distributed according to a Rayleigh distribution with mean upwelling rates of 20, 25, and 30 m $yr^{-1}$. A 10 000-yr-average deep-water temperature is shown for each value of $T_{atm}$. The dashed lines show results with steady upwelling, with upwelling rates of 50, 55, 60, and 65 m $yr^{-1}$.

the mean upwelling rate is not critical to determining deep-water temperature. Any upwelling distribution which allowed values above 60 m $yr^{-1}$ to occur 4% of the time would yield the same deep-water temperature. The constant case can be viewed as a very narrow distribution that also satisfies this requirement.

It is also seen from Fig. 4 that the variable upwelling cases differ further from the constant upwelling cases in that the deep-water temperature is sensitive to $T_{atm}$ over a wider range, extending both to higher and lower values of $T_{atm}$. This behavior results because the frequency of convection is not constant as a function of $T_{atm}$, as also seen for the constant upwelling case [Eq. (12)]. The upwelling rate that defines the threshold for convection therefore must vary as a function of $T_{atm}$.

This model extension illustrates that the main results derived previously apply under fluctuating upwelling, provided one interprets the neutral stability lines in Figs. 2 and 3 as being determined by some appropriate value of upwelling, near the high end of the frequency distribution of upwelling rate based on the required frequency of convection.

### b. Seasonally varying surface forcing

We next consider an extension of the model designed to explore the impact of seasonal variations in atmospheric forcing. This extension allows for explicit time dependence of the deep-water box via Eqs. (13) and (14) as well as explicit time dependence of the surface box according to

$$H\frac{dT_S}{dt} = Q_1(T_D - T_S) + K_0(T_{atm} - T_S) \quad (T_S \geq T_0), \quad \text{and} \tag{15}$$

$$H\frac{dS_S}{dt} = Q_1(S_D - S_S) - FS_0, \tag{16}$$

where $H$ is a fixed surface layer depth. Sea ice is implicitly represented by setting $T_S = T_0$ whenever $T_S$ would otherwise fall below the freezing point $T_0$. The convective fraction $f$ is allowed here to vary continuously, diagnosed based on the density difference $\Delta\rho = \alpha(T_S - T_D) - \beta(S_S - S_D)$ between the surface and deep box according to

$$\begin{aligned} f &= 1 && (\Delta\rho < 0), \\ f &= 1 - \Delta\rho/\Delta\rho_c && (0 \leq \Delta\rho < \Delta\rho_c), \quad \text{and} \\ f &= 0 && (\Delta\rho_c < \Delta\rho), \end{aligned} \tag{17}$$

where $\Delta\rho_c$ is a constant small density difference defining a threshold for convection. The approach conceptually divides the surface into stratified and convective regions with $f$ denoting the convective fraction. In the context of the bistability noted earlier, Eq. (17) has the effect of asserting a preference for a stratified state, as was also done explicitly for the analytical steady-state model considered previously. To keep the model as simple as possible, we neglect small terms related to entrainment and detrainment of deep water into the surface box (due to changes in $f$) and we neglect freshwater and latent heat effects due to growth and decay of sea ice. We solve the system by forward time stepping with a time step of 0.01 years using $H = 100$ m, $\Delta\rho_c/\alpha = 0.1$°C, $V_D/(AQ_1) = 200$ years, $Q_1 = 60$ m $yr^{-1}$, and other parameters from Table 1.

Figure 5 shows results for a 1000-yr run with $T_{atm}$ varying sinusoidally with a range of 10°C, a mean of −1°C, and a period of 1 year. Only the last 2 years are shown, by which time the system has achieved a quasi-steady state. In this state, surface water temperatures are at the freezing point for a several-month period characterized by a marginally stable surface layer ($\Delta\rho < \Delta\rho_c$) and convective cooling of deep water that counteracts the warming over the rest of the year. The period of freezing lags the seasonal cycle in $T_{atm}$ because of the finite adjustment time ($H/K_0$) of the surface layer.

The wintertime marginal stability is easily shown to result from essentially the same feedback loop on deep-water temperature as describe above for the steady analytical model. Using Eq. (7b) with $Q_1 = 60$ m $yr^{-1}$ and other parameters from Table 1, a deep-water temperature of $T_{max} = 1.733$°C is predicted by the steady analytical model, which can be compared to a mean deep-water temperature of ~1.645°C from the seasonal

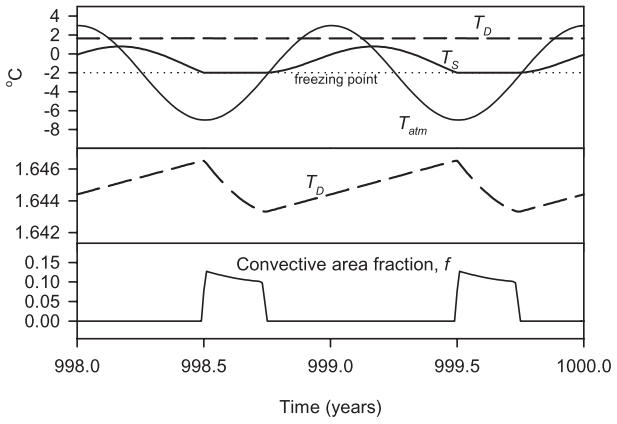


FIG. 5. Solutions to the model that include tendency terms for both deep and surface boxes with seasonal atmospheric forcing via $T_{\text{atm}}$. (top) Deep-water temperature $T_D$, surface water temperature $T_S$, and effective atmospheric temperature $T_{\text{atm}}$ are shown. (middle) Temperature range for $T_D$ is expanded. (bottom) Convective fraction is shown. Shown are the last two years of a 1000-yr model run.

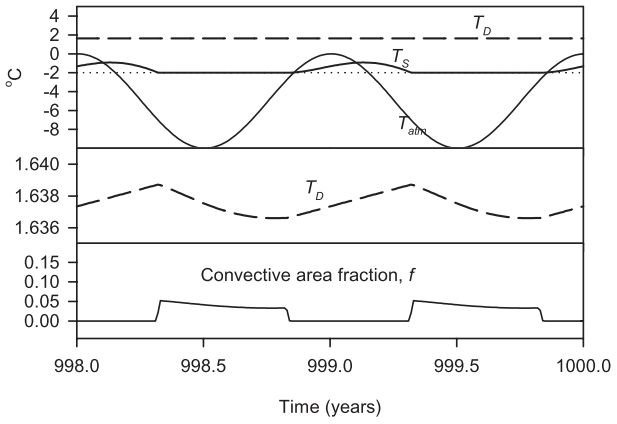


FIG. 6. As in Fig. 5, but with the model forced under colder atmospheric conditions (lower $T_{\text{atm}}$).

model. The offset of 0.088°C is explained by the threshold for convection having been shifted via Eq. (17) by $\Delta\rho_c/\alpha =$ 0.1°C, with a small adjustment because $f$ is nonzero in winter (requiring $\Delta\rho < \Delta\rho_c$).

Figure 6 shows results from a run which is identical except for colder atmospheric forcing ($T_{\text{atm}}$ cycling around −5°C instead of −1°C). Although the freezing/convective season is now longer, the steady-state deep-water temperature is only marginally lower than the warmer run. The insensitivity of deep-water temperature to atmospheric forcing is consistent with the behavior of the steady model when the surface is at the freezing point. In a seasonal model, the insensitivity is evidently tied to the occurrence of seasonal rather than year-round freezing. Additional runs (not shown), identical except for warmer atmospheric forcing, showed that the seasonal model also exhibits a nonfreezing regime where the system is marginally stable with convection in the coldest months and where $T_D$ is directly sensitive to $T_{\text{atm}}$. At even warmer conditions, convection ceases and $T_D$ is clamped at $T_N$ regardless of $T_{\text{atm}}$. These behaviors are also consistent with the steady model.

### c. Discussion of model extensions

These model extensions show that a feedback loop, similar to that which operates in the basic model, also operates across a broader ensemble of models with temporally varying forcing. As in the basic model, the feedback loop controls deep-water temperature to a set point, determined by upwelling rates, freshwater inputs, and thermal forcing in the south yielding intermittent convection (whether temporally or spatially) with a marginally stable surface layer. The main additional insight from these extensions is that the relevant southern forcing is not the temporal mean forcing but rather some appropriate average of extreme forcing. The model extensions explored stochastic upwelling and seasonally varying temperatures, but generally the combination of extreme upwelling, surface cooling, and weakest freshwater inputs must be considered in concert. The deep-ocean temperature in the intermittent convective steady state will be set by these extreme conditions. Thus, the appropriate values of $T_{\text{atm}}$, $Q_1$, and $F$, to use in Eq. (7) to determine $T_{\text{neut1}}$ (which equals the deep-water temperature in the intermittent convective steady-state conditions) are relatively extreme values, coinciding with some combination of maximum upwelling, maximum cooling conditions, and minimal freshwater inputs. The relevant range of extreme forcing is determined by the fraction of time that the system must convect to maintain a steady state. Below, we show that for the modern ocean, this fraction is around ~1%. Thus, assuming this feedback loop is relevant to the modern ocean, we would expect deep waters to be maintained at a temperature that allows the southern surface to convect under the most extreme ~1% of conditions. Although our model simulations considered only temporal variations in forcing, it is clear that spatial variations will also need to be considered in assessing extreme conditions in a more realistic model.

Despite the importance of extreme conditions for setting deep-ocean temperature and thresholds for convection, the average, rather than peak, upwelling rate is nevertheless also relevant to the problem, because it is the average upwelling that is linked to the turnover time of the deep ocean and thus controls the northern heat input to the deep ocean. Although this heat input does not regulate deep-ocean temperature in our model, it nevertheless determines the heat loss from the southern surface, and thus the frequency of convection. The pertinent upwelling

rate to use in Eq. (12) is thus the mean upwelling rate (not the peak rate). The need to distinguish peak from mean upwelling for different aspects of the problem is clearly critical to the extension to more realistic situations.

## 4. Further discussion

The model presented here shows how a surface layer with low static stability, such as that observed around Antarctica, can result from of a feedback loop involving deep-ocean temperature and intermittent convection. The feedback loop can operate over a range of climate states, thus suggesting that the close match between thermal and freshwater buoyancy forcing of the Antarctic surface may not be coincidental. The close match may be a symptom of the operation of this feedback loop. The feedback loop effectively regulates the thermal forcing in terms of the freshwater forcing, thus ensuring the match. This is achieved by partitioning the total air–sea heat flux between convective and stratified regions so that the heat flux in the stratified regions closely balances the net freshwater buoyancy flux.

Observations show that surface waters immediately south of the ACC experience net buoyancy gain, thus favoring the conversion of deep water which upwells along isopycnal surfaces into less dense water, such as Antarctic Intermediate Water (AAIW) or Subantarctic Mode Water (SAMW) (e.g., Speer et al. 2000). Further south, net buoyancy loss at the surface favors the conversion of upwelled waters into AABW. Both of these realms have analogs in our model (in the intermittent regime): AAIW/SAMW formation associated with the surface outflow (and its subsequent subduction); and AABW formation associated with regions of convection. It is tempting to assume that the division of the real ocean into these realms is controlled by the pattern of atmospheric forcing. The analogy with the box model, which has a uniform surface boundary condition, suggests another possibility: the buoyancy forcing in the two realms may be coupled so as to ensure the existence of a finite but small convective region, consistent with the requirement that deep-ocean temperature be in a quasi-steady state. This coupling would cause the buoyancy forcing in the stratified realm to be determined, not simply by the local atmospheric forcing, but linked remotely via deep-water temperature to the heat flux in the convective region. If the background ocean and atmospheric conditions are relatively uniform, this coupling can lead to a large surface region that is marginally stratified.

Recent studies using simple box models, but allowing for dynamic control of overturning based on density differences, have shown the possibility of deep decoupling oscillations (Colin de Verdière et al. 2006; Colin de Verdière 2007). This possibility is suppressed in our box model because the overturning rates are fixed. A key question is whether the feedback loop presented here is retained and whether oscillations become possible when dynamic overturning control is allowed. Addressing this question is complicated, however, given the need to account for both wind-driven and buoyancy-driven flows, as well as eddy effects. A further complication, clarified by the model extensions, is that it is not the mean upwelling rate but rather peak rates that are critical to setting deep-water temperature, suggesting that a spatially resolved model may be required to adequately address the question.

If the feedback loop on deep temperature is relevant to the real ocean, then deep-water temperatures should be roughly determined by the relation $T_D = T_0 + \beta S_0 F_1/\alpha Q_1$ as is appropriate for an ice-covered layer. We can check this relationship against parameters for the real ocean. Taking an average deep-water temperature of around 1.5°C, and other parameter values from Table 1, yields an upwelling rate of $Q_1 = 63$ m yr$^{-1}$. As discussed in the previous section, we expect this to correspond to upwelling rates near the high end of the distribution of variable upwelling. We do not have available estimates for comparison, but the estimate seems plausible in comparison to the mean upwelling rate of 45 m yr$^{-1}$ for the Weddell Sea (Gordon and Huber 1990), considering that higher upwelling rates are likely to prevail over sea mounts and continental shelves (Jacobs 1991; Kampf 2005). A slightly lower upwelling rate would be sufficient if convection occurs in a region of sea ice divergence, thus reducing the net surface freshwater input.

The model provides a basis [Eq. (12)] for making a rough estimate of the fraction of the Southern Ocean that must undergo convection to sustain deep waters at 1.5°C. For this estimate we will assume $T_{\rm atm} - T_{\rm neut1}$ is of order −6°C, corresponding to heat loss of ~200 W m$^{-2}$ for open-water winter conditions in the Antarctic (Gordon 1981) using $K_0$ from Table 1. As Eq. (12) is based on a deep-water heat budget, it depends on the mean, not peak upwelling rates. For $Q_1$ we adopt an estimate of the mean upwelling rate for the ocean south of the circumpolar current, and assume for simplicity that $Q_2 = 0$ m yr$^{-1}$. Adopting $T_{\rm neut1} = T_D = 1.5$°C and other parameter values from Table 1, we obtain $f \sim 0.0089$. If the convection is assumed to be confined to the coldest 3 months, the fraction of the total area undergoing convection in winter would be 4 times higher or around 3.6% of the total surface area south of the circumpolar current. The calculation shows that convection is a highly efficient cooling mechanism for deep waters and needs to be present only over a small fraction of the surface to cool the deep ocean to the set point. Although this result is reminiscent of fundamental arguments for

the smallness of ocean sinking regions (Stommel 1962; Beardsley and Festa 1972), it originates from different starting assumptions. In particular, the result applies to a system with wind-forced upwelling, whereas the earlier studies considered only buoyancy-driven flows.

Our model and its extensions did not consider the heterogeneity in the deep-ocean water masses and details of deep-ocean circulation. In the real ocean, the regions of deep southern upwelling and AABW formation are usually viewed as being spatially separated, with AABW formation occurring mostly on the Antarctic shelf regions, south of the main regions of upwelling, with a southward surface flow connecting these regions (Olbers and Visbeck 2005). These flows form the shallow half of the AABW overturning cell, whose deeper half involves the penetration of AABW into the ocean interior along the bottom, upwelling and mixing with NADW in the ocean interior, and return flow at middepth, feeding the upwelling and completing the loop (Olbers and Visbeck 2005). In our model, these processes are lumped together and considered as an instantaneous homogenization process driven by convection—obviously a gross simplification. The pertinent question here, however, is whether the feedback loop illustrated by the intentionally very simple model may also operate in the real ocean. The details of the formation and transport of AABW and the diapycnal mixing that drives deep upwelling (Naviera Garabato et al. 2004) are not obviously so important in this regard. Considering that AABW has a direct influence on deep-water temperatures, and that the deep-water temperature must influence AABW formation via the effects on stratification, it would seem that a similar feedback loop must be relevant as one factors controlling deep-water temperature in the real ocean. The details of the subsurface circulation are clearly relevant, however, for determining the time lag between the onset of Antarctic convection and its eventual impact on upwelled deep waters, which will influence the time scale over which the feedback loop operates, and whether it oscillates. From the slow turnover of global deep waters (Bolin and Stommel 1961), this time lag can be expected to be in the multicentury-to-millenial time scale.

Our basic model and its extensions also did not consider several other possible complications, such as the seasonal evolution of upper-ocean salinity (Martinson 1990), nonlinearities of the equation of state of seawater (Pierce et al. 1995), and complex dynamics that governs the real ocean–atmosphere system, such as eddy heat fluxes and impacts of air–sea fluxes on atmospheric conditions, etc. Such complications will need to be examined using more complete models.

Assuming deep-water temperatures in the real ocean are controlled by a mechanism similar to the box model, one can ask how the deep-ocean temperature would be expected to change in response to cooling of NADW, all else being fixed. Such a cooling process might be expected to occur at the onset of a glacial cycle, driven by orbital forcing in the Northern Hemisphere. Starting from the intermittent ice-covered regime (assumed to correspond to a modern-like state) the deep temperatures initially would be insensitive to cooling NADW because of a compensating reduction in Antarctic convection. On further cooling, however, a threshold would be reached when NADW cooled below the temperature of average deep waters (assumed to be initially set by the neutral stability criterion). From then on, Antarctic convection would be completely shut down, and the deep ocean would fill exclusively with (the colder) NADW. Interestingly, the modification of deep water upon cooling NADW involves three process all favorable to a reduction in the concentration of atmospheric carbon dioxide: (i) reducing the exposure of deep water to the atmosphere around Antarctica, (ii) filling the ocean with a source with low preformed nutrients, which increases the biologically-driven trapping of $CO_2$ in deep waters (Toggweiler et al. 2003), and (iii) and by increasing $CO_2$ solubility via cooling. Further cooling would likely eventually lead to situations beyond the scope of the present analysis, however, due to the increased importance of long-distance ice transport in a colder climate.

One can also ask how the feedback mechanism might be relevant in the context of future global warming. Coupled models suggest that Antarctic convection may decrease over the next few centuries because of global warming–induced freshening and warming of surface waters at high southern latitudes (e.g., Matear and Hirst 2003). Although the feedback mechanism would be expected to partly stabilize the system against perturbations that act over time scales similar or longer than the effective turnover time of deep waters, the perturbations due to increasing greenhouse gases are too fast for this to occur. On the decadal-to-century time scale of greenhouse gas–induced global warming, the deep-ocean temperature will not be able to keep pace with the freshening and warming of surface waters. Indeed, because the feedback loop may have preconditioned water column to be in a marginally stable state, the system may be especially sensitive to perturbations. A decrease in convection is thus consistent with the feedback mechanism.

*Acknowledgments.* This work was carried out in part while RK was on sabbatical leave at the Leibniz Institute of Marine Sciences in Kiel, supported by the Humboldt Foundation and the Cluster of Excellence ‘‘Future

Ocean.'' We thank two anonymous reviewers for very helpful comments.

## REFERENCES


Adkins, J. F., K. McIntyre, and D. P. Schrag, 2002: The salinity, temperature, and $d^{18}O$ of the glacial deep ocean. *Science,* **298,** 1769–1773.

Beardsley, R., and J. Festa, 1972: A numerical model of convection driven by a surface stress and non-uniform horizontal heating. *J. Phys. Oceanogr.,* **2,** 444–455.

Bolin, B., and H. Stommel, 1961: On the abyssal circulation of the World Ocean—IV. Origin and rate of circulation of deep ocean water as determined with the aid of tracers. *Deep-Sea Res.,* **8,** 95–110.

Colin de Verdière, A., 2007: A simple model of millennial oscillations of the thermohaline circulation. *J. Phys. Oceanogr.,* **37,** 1142–1155.

——, M. Ben Jelloul, and F. Sevellec, 2006: Bifurcation structure of thermohaline millennial oscillations. *J. Climate,* **19,** 5777–5795.

Foster, T. D., and E. C. Carmack, 1976: Frontal zone mixing and Antarctic Bottom Water formation in southern Weddell Sea. *Deep-Sea Res.,* **23,** 301–317.

Gildor, H., and E. Tziperman, 2001: The physics behind biogeochemical glacial-interglacial $CO_2$ variations. *Geophys. Res. Lett.,* **28,** 2421–2424.

Gnanadesikan, A., 1999: A simple predictive model for the structure of the oceanic pycnocline. *Science,* **283,** 2077–2079.

Gordon, A. L., 1981: Seasonality of Southern Ocean sea ice. *J. Geophys. Res.,* **86,** 4193–4197.

——, 1991: The Southern Ocean: Its involvement in global change. *Proc. Int Conf. on the Role of Polar Regions in Global Change,* Fairbanks, AK, University of Fairbanks, Alaska.

——, and B. A. Huber, 1990: Southern Ocean winter mixed layer. *J. Geophys. Res.,* **95,** 11 655–11 672.

——, ——, H. H. Hellmer, and A. Ffield, 1993: Deep and bottom water of the Weddell Sea's western rim. *Science,* **262,** 95–97.

——, M. Visbeck, and J. C. Comiso, 2007: A possible link between the Weddell Polynya and the Southern Annular Mode. *J. Climate,* **20,** 2558–2571.

Haarsma, R. J., J. D. Opsteegh, F. M. Selten, and X. Wang, 2001: Rapid transitions and ultra-low frequency behavior in a 40-kyr integration with a coupled climate model of intermediate complexity. *Climate Dyn.,* **17,** 559–570.

Haney, R. L., 1971: Surface thermal boundary condition for ocean circulation models. *J. Phys. Oceanogr.,* **1,** 241–248.

Jacobs, S. S., 1991: On the nature and significance of the Antarctic slope front. *Mar. Chem.,* **35,** 9–24.

Johnson, G. C., 2008: Quantifying Antarctic Bottom Water and North Atlantic Deep Water volumes. *J. Geophys. Res.,* **113,** C05027, doi:10.1029/2007JC004477.

Kampf, J., 2005: Cascading-driven upwelling in submarine canyons at high latitudes. *J. Geophys. Res.,* **110,** C02007, doi:10.1029/2004JC002554.

Karsten, R., H. Jones, and J. Marshall, 2002: The role of eddy transfer in setting the stratification and transport of a circumpolar current. *J. Phys. Oceanogr.,* **32,** 39–54.

Keeling, R. F., and B. B. Stephens, 2001: Antarctic sea ice and the control of Pleistocene climate instability. *Paleoceanography,* **16,** 112–131, 330–334.

Lenderink, G., and R. J. Haarsma, 1994: Variability and multiple equilibria of the thermohaline circulation associated with deep-water formation. *J. Phys. Oceanogr.,* **24,** 1480–1493.

Lumpkin, R., and K. Speer, 2007: Global ocean meridional overturning. *J. Phys. Oceanogr.,* **37,** 2550–2562.

Martinson, D. G., 1990: Evolution of the Southern Ocean winter mixed layer and sea ice–open ocean deep-water formation and ventilation. *J. Geophys. Res.,* **95,** 11 641–11 654.

Matear, R. J., and A. C. Hirst, 2003: Long-term changes in dissolved oxygen concentrations in the ocean caused by protracted global warming. *Global Biogeochem. Cycles,* **17,** 1125, doi:10.1029/2002GB001997.

Meissner, K. J., M. Eby, A. J. Weaver, and O. A. Saenko, 2008: $CO_2$ threshold for millennial-scale oscillations in the climate system: Implications for global warming scenarios. *Climate Dyn.,* **30,** 161–174.

Naviera Garabato, A. C., K. L. Polzin, B. A. King, K. J. Heywood, and M. Visbeck, 2004: Widespread intense turbulent mixing in the Southern Ocean. *Science,* **303,** 210–213.

Olbers, D., and M. Visbeck, 2005: A model of the zonally averaged stratification and overturning in the Southern Ocean. *J. Phys. Oceanogr.,* **35,** 1190–1205.

Orsi, A. H., S. S. Jacobs, A. L. Gordon, and M. Visbeck, 2001: Cooling and ventilating the abyssal ocean. *Geophys. Res. Lett.,* **28,** 2923–2926.

Pierce, D. W., T. P. Barnett, and U. Mikolajewicz, 1995: Competing roles of heat and freshwater flux in forcing thermohaline oscillations. *J. Phys. Oceanogr.,* **25,** 2046–2064.

Saenko, O. A., A. Schmittner, and A. J. Weaver, 2002: On the role of wind-driven sea ice motion on ocean ventilation. *J. Phys. Oceanogr.,* **32,** 3376–3395.

Sigman, D. M., and E. A. Boyle, 2000: Glacial/interglacial variations in atmospheric carbon dioxide. *Nature,* **407,** 859–869.

——, M. P. Hain, and G. H. Haug, 2010: The polar ocean and glacial cycles in atmospheric $CO_2$ concentration. *Nature,* **466,** 47–55.

Speer, K., S. R. Rintoul, and B. Sloyan, 2000: The diabatic Deacon cell. *J. Phys. Oceanogr.,* **30,** 3212–3222.

Stommel, H., 1961: Thermohaline convection with two stable regimes of flow. *Tellus,* **13,** 224–230.

——, 1962: On the smallness of sinking regions in the ocean. *Proc. Natl. Acad. Sci. USA,* **48,** 766.

Stössel, A., K. Yang, and S. J. Kim, 2002: On the role of sea ice and convection in a global ocean model. *J. Phys. Oceanogr.,* **32,** 1194–1208.

Talley, L. D., J. L. Reid, and P. E. Robbins, 2003: Data-based meridional overturning streamfunctions for the global ocean. *J. Climate,* **16,** 3213–3226.

Toggweiler, J. R., and B. Samuels, 1995a: Effect of Drake Passage on the global thermohaline circulation. *Deep-Sea Res. I,* **42,** 477–500.

——, and ——, 1995b: Effect of sea ice on the salinity of Antarctic bottom waters. *J. Phys. Oceanogr.,* **25,** 1980–1997.

——, R. Murnane, S. Carson, A. Gnanadesikan, and J. L. Sarmiento, 2003: Representation of the carbon cycle in box models and GCMs—2. Organic pump. *Global Biogeochem. Cycles,* **17,** 1027, doi:10.1029/2001GB001841.

Walin, G., 1993: On the formation of ice on deep weakly stratified water. *Tellus,* **45A,** 143–157.

Welander, P., 1982: A simple heat salt oscillator. *Dyn. Atmos. Oceans,* **6,** 233–242.

Winton, M., and E. S. Sarachik, 1993: Thermohaline oscillations induced by strong steady salinity forcing of ocean general circulation models. *J. Phys. Oceanogr.,* **23,** 1389–1410.

Zwally, H. J., and Coauthors, 1983: *Antarctic Sea Ice, 1973–1976: Satellite Passive-Microwave Observation*. NASA, 206 pp.